Journal of Computational and Applied Mechanics, Vol. 7., No. 1., (2006), pp. 23–39

EXPERIMENTAL AND NUMERICAL BIOMECHANICAL ANALYSIS OF THE HUMAN LUMBAR SPINE

Márta Kurutz
Department of Structural Mechanics
Budapest University of Technology and Economics
H-1521 Budapest, Hungary
kurutzm@eik.bme.hu

Béla Fornet
International Medical Center
Dózsa Gy. út 112., H-1062 Budapest, Hungary

Miklós Gálos[1], Árpád Tornyos[2] and Tibor Szabadszállási[2]
[1]Department of Building Materials, [2]Department of Structural Mechanics
Budapest University of Technology and Economics
H-1521 Budapest, Hungary
mgalos@freemail.hu

[Received: October 16, 2004]

Abstract. A survey of biomechanical research of the human lumbar spine is presented, conducted by the research group of the Department of Structural Mechanics and the Research Centre for Biomechanics of the Budapest University of Technology and Economics. A complex biomechanical analysis of the human lumbar spine is performed, aimed partly to improve the efficiency of conservative traction therapies and partly to prevent osteoporosis. The former concerns tension, the latter compression of the lumbar spine. As for tension, time-related in vivo elongations were measured during the regular traction hydrotherapy of patients. Based on the experimental results, parameter-dependent viscoelastic numerical tensile models of the lumbar functional spinal units were created for numerical simulation and parameter identification. As for compression, in vitro compression tests were executed for lumbar vertebral bodies, together with measuring bone mineral density and trabecular morphometry, to determine the relations between compressive load bearing capacity and bone architecture. In this paper a survey of these experimental and numerical approaches of biomechanics of the human lumbar spine is reported.

Keywords: human lumbar spine, discs, vertebrae, in vivo elongations, creep, numerical simulation, parameter identification, in vitro compression, morphometry

1. Introduction

The present paper gives a survey of the recent results on biomechanical spine research conducted by the research group of the Department of Structural Mechanics and the Research Centre for Biomechanics at the Budapest University of Technology and

Economics. The first part of the report is related to the biomechanics of lumbar traction, to improve the efficiency of conservative traction therapies. The second part is focussed on the biomechanics of lumbar compression, to contribute to the research of osteoporosis.

The goal of the study of lumbar traction was to create a time-related numerical tensile model of human lumbar-lumbosacral motion segments for the numerical simulation of traction therapies. The model has been based on a large-scale experimental analysis of elongations of human lumbar segments in pure centric tension. Time-dependent in vivo elongations of segments L3-L4, L4-L5 and L5-S1 have been measured during the usual traction hydrotherapy of patients, by using a subaqual ultrasound measuring method documented by Kurutz et al. in [1,2]. Elongations of segments were considered to be changes in the distance between two neighbouring spinous processes. Based on the measured elongations of segments in terms of certain biomechanical parameters, parameter-dependent numerical lumbar-lumbosacral L3-S1 FSU models have been created for the numerical simulation and parameter-identification of human lumbar spine segments in traction therapies. 2D and 3D FEM models were created, and the global elongations of FSUs were used for identification of the local material parameters of the component organs of lumbar spine segments.

The goal of the study of lumbar compression was to give the relations between the mechanical properties and bone architecture of human lumbar vertebral bodies, in the framework of osteoporosis research. Image analyses, CT, MR, densitometry and mechanical tests were executed for the lumbar vertebral bodies, to clarify the relations between the compressive load bearing characteristics and bone architecture, in terms of aging and sex. The compressive strength of cadaver lumbar vertebrae was determined by mechanical tests, and the bone architecture was analyzed in CT images. A one-way compressive test was carefully performed on each vertebra up to collapse. The automatically plotted load-displacement diagrams were classified and linearized. Age- and sex-related functions and trends of both strength characteristics and vertebral architecture were obtained for different life periods of osteoporotic elderly. As compressive strength parameters, limit stresses and strains, Young's moduli, proportional stresses and strain limits, ductility and energy absorption capacity were calculated for the lumbar vertebrae L1 and L2, in terms of aging and sex.

In this paper the recent results on biomechanics of lumbar traction and compression are presented.

2. Numerical simulation and parameter identification of lumbar traction

2.1. **Introductory remarks.** Based on the measured elongations of lumbar segments during traction hydrotherapy, parameter-dependent numerical lumbar-lumbosacral FSU models have been created for the numerical simulation of traction treatments.

Suspension hydrotherapy is a Hungarian invention, introduced and described by Moll [4,5,6], and later by Bene [7], while the biomechanics of the therapy has been

detailed by Bene and Kurutz [3]. During the traction bath treatment, patients are suspended cervically or by armpit supports in lukewarm water for 20 minutes, loaded by extra lead weights applied on the ankles. In our experiments, cervical suspension has been applied exclusively, since this mode of support provides the most effective stretching load to the lumbar part of the spine, moreover, in this case the effect of muscles can be practically neglected.

2.2. **Force effects in traction hydrotherapy.** Tensile load effects depend on the definition of the tensile deformations. By definition, tensile deformations of segments suspended in water are considered to be a decrease of compressive deformations existing before the treatment. Namely, zero deformation belongs to the common compressed state of segments of the normal upright position of the body. Tensile deformation of segments has been considered to be the change in distance between two spinous processes of neighboring vertebrae.

In the case of cervical suspension, three load effects cause traction deformations along the spinal column: 1. the decompressive force as the removal of the compressive load of the body weight existing before the treatment; 2. the active tensile force due to buoyancy; 3. the extra loads applied for the therapy. In the case of free cervical suspension in water, the effect of muscles can be neglected. The distribution of these traction load effects is illustrated in Figure 1. The compressive loads of the upright standing position are seen to the left of the vertical zero axis, while the active tensile loads of suspension are illustrated to the right.

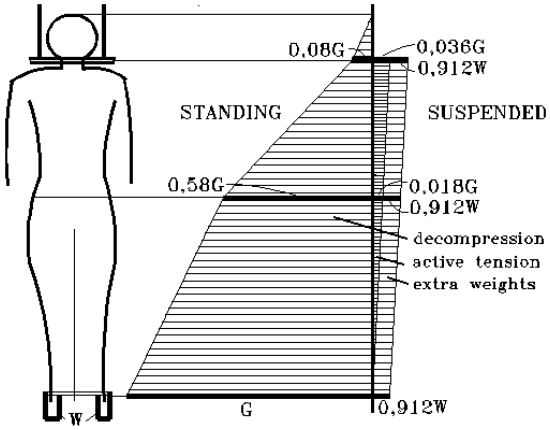

Figure 1. Forces in traction hydrotherapy

The decompressive force is equal to the compressive load acting on the spine before the treatment, in normal upright standing position. This gravitation force increases downwards continuously, starting from zero, namely from the top of the head to the floor, where the total weight G of the body acts. At the cervical level, this force is equal to the weight of the head, that is, about 8% of the body weight. At the lumbar level the decompressive force takes about 58-60 % of the body weight, namely, the

weight of the head and trunk together. That is, $F_1 = 0.58G$, seen in Figure 1. For a patient of weight of $G = 700N$, the decompressive force at the lumbar level is about $F_1 = 0,58G = 406N$.

The active tensile force has been calculated in the paper of Bene and Kurutz [3]. It depends on the buoyancy, decreasing continuously along the spinal column, starting from the suspending point where the force has its maximum value, seen in Figure 1. According to [3], being suspended cervically in water without any artificial weights, the value of the active tensile force acting at the suspension point is about

$$0.92G(1 - \rho_w/\rho_b) ,$$

where ρ_w and ρ_b are the density of water and the human body, respectively. By considering half of this force at the lumbar level, the active lumbar tensile force reads

$$F_2 = 0.46G(1 - \rho_w/\rho_b) .$$

By considering an average human body-density

$$\rho_b = 1040\ kg/m^3$$

and a normal water density

$$\rho_w = 1000\ kg/m^3 ,$$

it yields

$$F_2 = 0.46G(1 - \rho_w/\rho_b) = 0,018G ,$$

seen in Figure 1. For example, in the case of a patient of $G = 700\ N$ body weight, the lumbar active tensile force yields only

$$F_2 = 0.018 \cdot 700\ = 12,6\ N\ .$$

Thus, the active tensile load seems to be surprisingly low.

The extra weight loads are applied to provoke a more intensive stretching effect in the lumbar spine. The extra weight load depends on the value, specific weight and the application position of the extra lead weights, detailed also in [3]. Since the extra lead weights are also in the water, their original value W is reduced to

$$F_3 = W\ (1 -\ \rho_w/\rho_l) ,$$

due to the buoyancy. By considering the density of the lead to be

$$\rho_l = 11\ 350\ kg/m^3 ,$$

the extra weight load yields

$$F_3 = W\ (1 -\ \rho_w/\rho_l) = 0.912\ \mathrm{W} ,$$

seen in Figure 1. Thus, by substituting the applied $2 \cdot 20N$ actual weights, that is, $W = 40N$, we obtain

$$F_3 = 0.912 \cdot 40 = 36.48N .$$

During the traction bath treatment, the sum of the detailed three tensile forces is to be considered:

$$F = F_1 + F_2 + F_3 = 0.58G + 0.018G + 0.912W\ = 0.598\mathrm{G} + 0.912\mathrm{W} ,$$

as seen in Figure 1, by assuming the above-considered densities. By comparing the three component forces, obviously, the dominant stretching load is the decompressive force, if applying cervical suspension. It takes about 97% of the stretching load if no extra loads are applied.

2.3. **Parameter-dependent viscoelastic numerical models of lumbar segments.** Elongation values of lumbar segments L3-4, L4-5 and L5-S1 have been measured. More than 400 lumbar segments of 155 patients have been measured, more than 3000 ultrasound images have been evaluated. The 155 measured subjects have been divided into two groups: 88 patients of less degenerated segments with medically prescribed extra loads, and a group of 67 patients with more degenerated segments without any extra loads. This latter group consisted of patients for whom the extra lead loads have been contraindicated due to certain degeneration of the lumbar segments or discs. Tensile deformability of lumbar segments was measured and evaluated in terms of biomechanical parameters, like sex, aging, body weight and height and body mass index.

Based on the experimental results of lumbar segments L3-4, L4-5 and L5-S1, a so-called general lumbar FSU model L3-S1 has been created for numerical simulations. The functional spinal unit (FSU) consists of two adjacent vertebrae with the disc between them and the related soft tissues, like ligaments, tendons and muscles. FSU model L3-S1 is valid for the lumbar part between segments L3 and S1.

Just being suspended (t=0 min), due to the removal of compression and the buoyancy, unloading of discs and segments occur, thus, even without any extra weights, significant extension was registered. These elongations correspond to the elastic behaviour of segments with a mean value of 0.4-0.8 mm for males, 0.3-0.4 mm for females. Suspended with extra weights (t=3min), 0.6-1.0 mm mean elastic elongations were registered for men, and 0.5-0.8 mm for women. At the end of the treatment (t=20 min), the total mean elongations were 0.9-1.4, and 0.8-1.3 mm with extra loads, and 0.7-1.0 mm and 0.7-0.8 mm without extra weights for men and women, respectively. During the treatment, both the ratio and the value of deformability increased with a decreasing tendency in distal direction.

By considering aging effects, three age groups can be distinguished: young under 40 years, middle aged between 40-60 years and old over 60 years, seen in Figure 2. For the lumbar segment model of less degenerated segments, the mean instant elastic deformations (t=0 min) decrease with aging: 0.90, 0.59, 0.26 mm for males; 0.66, 0.39, 0.21 mm for females; and 0.82, 0.48, 0.23 mm for the whole group, for the three age groups, respectively. At the end of the treatment (t=20 min) the mean deformations decrease with aging again: 1.54, 1.17, 0.37 mm for males; 1.47, 1.19, 0.65 mm for females; and 1.51, 1.19, 0.55 mm for the whole group. The mean final deformations (t=20 min) also decrease with aging, for both males and females. There is no significant difference in age-dependence between men and women. However, the slope of the deformability decrease is slightly larger with increasing treatment time.

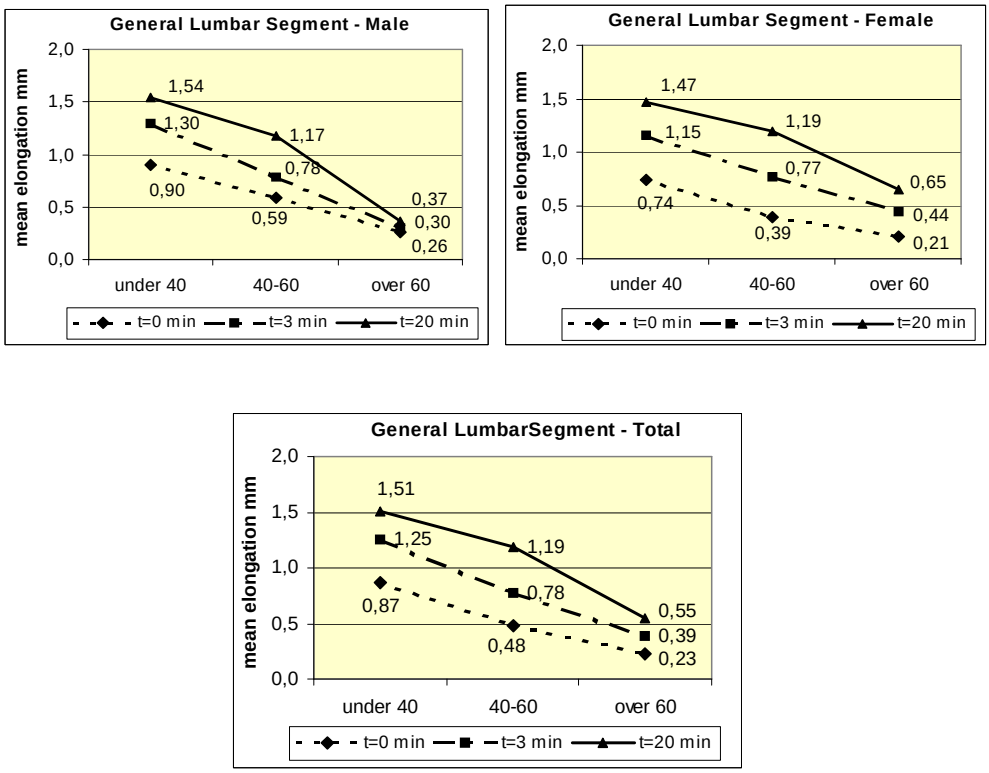

Figure 2. The three parameter spring-dashpot creep model

Since the traction load was constant during the 20 minute-long treatment, a typical creeping process developed and could be documented numerically. The creep process has been measured in the group of patients with less degenerated segments, loaded by 20-20 N extra weights on ankles. For the viscoelastic numerical model, the Poynting-Thomson type three-parameter spring-dashpot model has been used, seen in Figure 3, where spring constants represent the elastic properties and damping coefficients

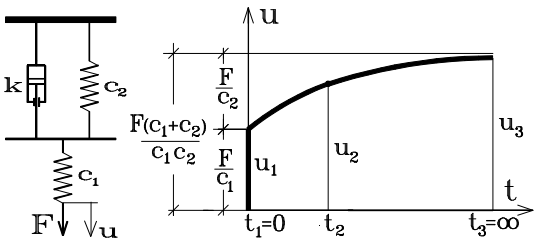

Figure 3. The three parameter spring-dashpot creep model

concern creep effects. The creep function, namely, the deformation in terms of time under constant load yields:

$$u = \frac{F}{c_2}\left(\frac{c_1 + c_2}{c_1} - e^{-c_2 \frac{t}{k}}\right) = \frac{F}{c_2}\left(\frac{c_1 + c_2}{c_1} - e^{-\frac{t}{T}}\right), \qquad T = k\frac{1}{c_2}$$

where T is the time constant. The parameters in this function, namely, the spring constants c_1 and c_2, and the damping coefficient k, were determined by the time-related in vivo measurements. In this way, three elongations have been obtained, from which the parameters of the function u could be calculated. Here we assumed that the last stage at the 20^{th} minute of the treatment concerns the steady state of the creep process. Creep functions of the general lumbar FSU model have been obtained in terms of sex, aging and other parameters.

Table 1. Sex-related parameters and creep moduli of general lumbar FSU model L3-S1

General Lumbar FSU Model LIII-SI				
extra weight 20-20N	units	male	female	total
segments	number	108	128	236
mean age	years	47.9	51.7	50.0
mean body weight	N	758	671	711
mean body height	cm	175	164	169
mean BMI	kg/m^2	24.9	25.1	25.0
elong. at t=0 min u_1	mm	0.66	0.43	0.52
elong. at t=3 min u_2	mm	0.83	0.74	0.78
elong. at t=20min u_3	mm	1.15	1.11	1.13
Creep parameters				
spring coeff. c_1	N/mm	742	1018	887
spring coeff. c_2	N/mm	999	643	756
damping coeff. k	Ns/μm	422	190	245
time constant T	min	7.04	4.93	5.40

Table 1 illustrates the creep moduli of the general lumbar FSU model for numerical purposes, by distinguishing between the sexes. The model is based on the mean values of 108 male, 128 female segments, and overall 236 segments. The mean initial elongation in women is about 66% of the deformation in men. However, the final deformations are quasi equal, since the damping in men is more than double that of women. Spring coefficient c_1 is equal to the initial tensile stiffness. This fact is obvious, by considering the mechanical model seen in Figure 3.

Initial tensile stiffness in males is about 750 N/mm, in females it is about 1000 N/mm. The damping coefficient in males is about 400 Ns/μm, in females it is about 200 Ns/μm. Consequently, after an initially smaller deformability in females, larger creep elongations occur. The final viscoelastic elongations are quasi equal.

Table 2. Age-related parameters and creep moduli of general lumbar FSU model L3-S1

General Lumbar FSU Model LIII-SI				
extra weight 20-20 N	units	under 40 yrs	40-60 years	over 60 yrs
segments	number	35	161	40
mean age	years	26.5	50.7	67.5
mean body weight	N	713	721	670
mean body height	cm	176.7	169.0	160.3
mean BMI	kg/m^2	22.9	25.2	26.0
elongation, t=0 min, u_2	mm	0.94	0.52	0.25
elongation, t=3 min, u_2	mm	1.25	0.78	0.39
elongation, t=20 min, u_2	mm	1.51	1.19	0.55
Creep parameters				
spring constant c_1	N/mm	492	899	1748
spring constant c_2	N/mm	812	698	1456
damping coefficient k	Ns/μm	186	256	417
time constant T	min	3.82	6.11	4.77

Creep behaviour of the general lumbar segment model L3-S1 is significantly different in terms of aging, as seen in Table 2, considering the three age groups. It was numerically verified that the initial stiffness increases, consequently, deformability decreases with aging,. Similarly, damping coefficients also increase, thus, creep deformability decreases with aging. These tendencies are valid for both sexes.

2.4. **Numerical simulation in traction.** As the first step of the numerical simulation, we checked the measured elongations by a simple 2D FEM model. Since the healthy spine segment is a symmetrical structure, the simple 2D model was related to the sagittal plane of the FSU. For the material constants we used the results by Antosik et al. [9] and Ciach et al. [10,11]. For the Young's moduli E and Poisson ratio í, the following data were used. For the vertebral cancellous bone E=1000 MPa and í=0.4, for the vertebral cortical bone E=15000 MPa and í=0.4, for the disc annulus E=5 MPa, í=0.35, for the disc nucleus E=1 MPa, í=0.49, for ligaments E=40 MPa and í=0.35 were considered.

The geometrical data of the FSU were obtained by measuring a typical lumbar segment. The height of a vertebra (including end-plates) was 25 mm, the height of the disc was 8 mm. The end-plates (containing both vertebral and disc bony end-plates) was 3 mm. The support of the structure was along the inferior surface of the lower vertebra. The load was distributed along the superior surface of the upper vertebra.

For the general behaviour of the segment complex, we assumed a bilinear material law. We assumed that the decompression takes place by large stiffness that is valid for compression, and for the active tension and extra weights, we assumed a smaller stiffness. Thus, 500 MPa for compression and 5 MPa for tension were applied as disc moduli.

In the loading phase of decompression, we applied 400 N that caused about 0.1 mm (0.097 mm) segment elongation. For the active tensile load and extra lead weight load together, we applied 49 N. The additional elongation was about 0.5 mm. These results were in good agreement with our measured elongations.

The numerical simulation confirmed our suspicion that in spite of the fact that the active tensile forces compared with the decompressive forces are very small, even a small value of extra weight load can cause a large elongation in the spine segment and disc. Thus, extra loads should be handled very cautiously.

As the second step of the numerical simulation, we refined the 2D FEM model to simulate the viscoelastic creep process, by applying NASTRAN software. For the viscoelastic numerical model, the Poynting-Thomson type three-parameter spring-dashpot models were used. Creep behaviour and creep curves of the general lumbar segment model L3-S1 were significantly different in terms of aging and sex.

For parameter identification, the NASTRAN model has been improved to a 3D configuration of FSU. The segment model has 35 000 nodal points with the relating 110 000 equations. Figure 4 illustrates the mesh of the FSU-model and the mesh of the component organs: cross-section of vertebrae, the disc and the separated ligaments.

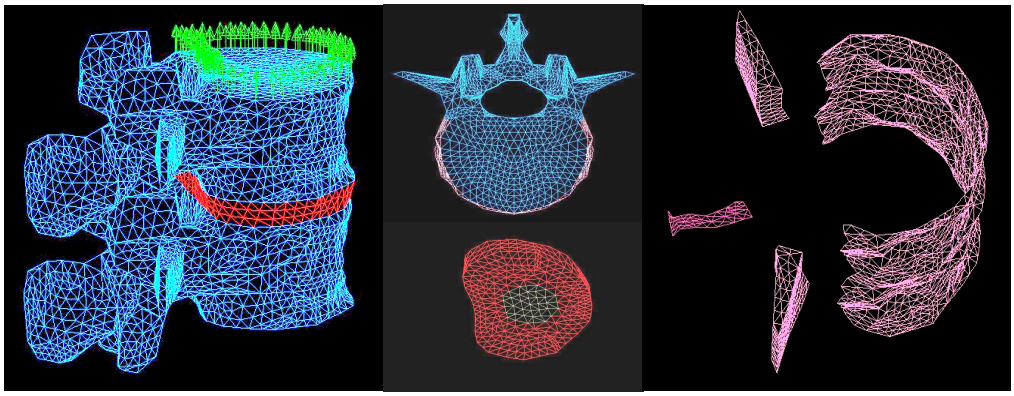

Figure 4. FEM mesh of the FSU model, vertebrae, disc and ligaments

Parameter identification aims to determine the in vivo controlled tensile behaviour and tensile material moduli of the component organs of lumbar segments that are completely missing in the international literature. Namely, except for the results of Kurutz et al. [1,2,3] there can hardly be found any experimental results for in vivo human lumbar spine in pure centric tension, when the effect of muscles are excluded. In the parameter identification process, the in vivo measured global elongations of the lumbar segment complex are used for control parameters in determining the material moduli of the local component organs. In this process, the material moduli of certain organs are kept constant while the material parameters of other organs are considered to be the variables of the problem. Under these parameters, numerical simulation is investigated, and those results are considered to be realistic and are accepted that

lead to the in vivo measured elongations. The intervals of material moduli used in parameter identification are as follows: cortical bone 1-20GPa, trabecular bone: 50-1000 MPa, disc annulus 5-500 MPa, disc nucleus 1 MPa, ligaments 10-100 MPa.

The parameter analysis shows that Young's modulus of the annulus has a significant effect on the deformability of the segment complex, and we can hardly assume that the tensile elastic modulus of the annulus is far smaller than the compressive one. This result seems to be evident since the basic property of the annulus is its resistance to compression. Another observation is that changing the stiffness of the cortical bone has no significant effect on the deformability of segments. However, the Young's modulus of the annulus has practically no effect on the stresses occurring in the cortical or trabecular bone, however, it has a significant effect on the stresses of the nucleus and annulus itself.

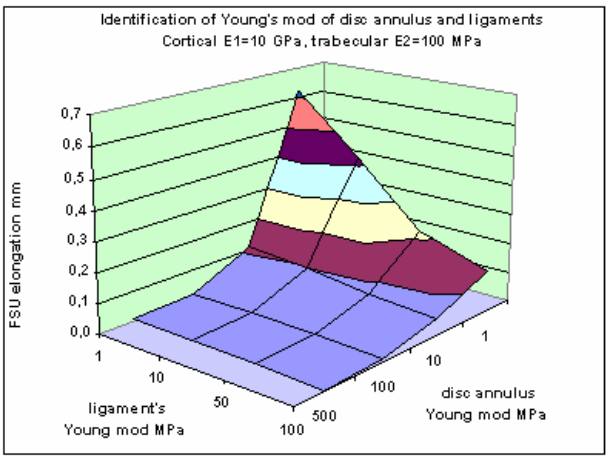

Figure 5. Parameter-identification of Young's moduli of disc annulus and ligaments

In Figure 5 the global elongation of the segment complex is illustrated in terms of the Young's moduli of the disc annulus and the ligaments. By considering the in vivo measured elongation, for example, to be 0.3 mm, the level of this elongation can be projected to the basic coordinate plane to show the possible coincidence of the real Young's moduli of the above mentioned organs.

3. Compressive strength and bone architecture of lumbar vertebrae

Compressive strength of cadaver lumbar vertebrae was determined by mechanical tests, and their bone architecture was analyzed by CT images. Age-related functions and trends of both strength characteristics and vertebral architecture were obtained for different life periods of the osteoporotic elderly.

54 cadaver lumbar L1 and L2 vertebrae without posterior elements were obtained from the spines of 16 males and 38 females. The age of males was between 47-87

years (mean age 65.6 year); the age of females was between 43-93 years (mean age 74.2 year).

Before mechanical testing, areal bone mineral density (aBMD in g/cm^2), CT and MRI analysis were performed for each vertebra. The CT images were used to analyze the bone architecture, to measure the diameters, the distribution and density of trabeculae. The measurements have been repeated in the coronal and sagittal plane and in the horizontal cross-sectional plane of vertebrae.

For mechanical testing, the two end-plates of vertebrae were cleared away, so that the upper and lower planes of vertebrae were parallel and smooth. In this way, the original height of vertebrae decreased by two times 1-4 mm. The reduced height and the upper and lower cross-sectional areas were measured and registered. The average of the two measured cross-sectional areas has been considered to be the cross sectional area of each vertebra.

A one-way compressive test was carefully performed on each vertebra up to the collapse. No cyclic loading and no unloading were performed. The measuring limit of the tester was 12.5 kN with accuracy of 3%. Compressive deformations were measured in three points, by angle of 120 degree from each other, with 0-5 mm measuring limit.

The automatically plotted load-displacement diagrams were linearized, and the related stress-strain diagrams were classified.

3.1. **Experimental compressive strength characteristics of lumbar vertebrae.** Table 1 contains the mean values of the given material or geometrical properties and the measured mechanical characteristics of vertebrae L1 and L2, by distinguishing between sexes. The mean values of areal BMD verify that the analyzed vertebrae belong to the osteoporotic class.

Table 3. Mechanical characteristics of lumbar vertebrae L1-L2 in compression

Lumbar vertebrae L1-L2		Males	Females	Total
Mean age	years	65.6	74.2	71.7
Areal bone mineral density (aBMD)	g/cm^2	0.446	0.347	0.376
Cross sectional area of vertebrae	mm^2	1609	1359	1436
Height of specimen without end-plates	mm	21.9	19.0	19.9
Break load	N	4322	2437	2995
Proportional stress	MPa	2.0	1.3	1.5
Proportional strain	%	3.3	2.9	3.0
Young's modulus	MPa	91	67	74
Limit stress	MPa	2.7	1.9	2.1
Limit strain, ductility	%	5.0	4.9	4.9
Energy absorption capacity	Joule	1.63	0.97	1.18

It can be seen that there is a significant difference in the load bearing properties of males and females, namely, the compressive load bearing capacity of women is about 30% smaller than that of men. The break load of women is 40-50% smaller than that of men. Moreover, since the cross-sectional areas of women are only 15%

smaller, consequently, both the proportional and limit stresses are 30-40% smaller in women than in men. The limit stresses were about 2.7 MPa for men, and 1,9 MPa for women. Young's moduli of women are about 20-30% smaller than that of men. At the same time, there is no significant difference between the sexes in the proportional or limit strains and in duclility. The proportional strains are equally about 3%, the limit strains are equally about 5%. However, there is a significant difference again in the energy absorption capacity of men and women: women have about 1 Joule, namely 35-45% smaller absorption capacity than men with 1.6-1.7 Joule. This comes partly from the smaller limit stresses and partly from the smaller volume of vertebrae of females.

Lindahl [13] and Hansson et al. [12] presented the main compressive strength characteristics of the cancellous bone of lumbar vertebrae. The proportional stress was 1.37-4.0 MPa, the proportional strain 6.0-6.7%, Young's modulus 22.8-55.6 MPa, the limit stress 1.55-4.60 MPa, and the limit strain was 7.4-9.5%. These results concern the cancellus core of vertebrae, proving that due to the high ductility, there is the trabecular bone that is responsible for the energy absorption ability of vertebrae to avoid injury in the case of an accidental dynamical load. Based on compressive tests of lumbar vertebrae, Tanaka et al. [18] found the value of limit stress between 0.14-4.54 MPa.

Figure 6 illustrates the linear approximation of the age-related decline of limit stresses of vertebrae L1-L2, between 43-93 years, by distinguishing between the sexes. A similar tendency has been found for the other strength parameters, as well.

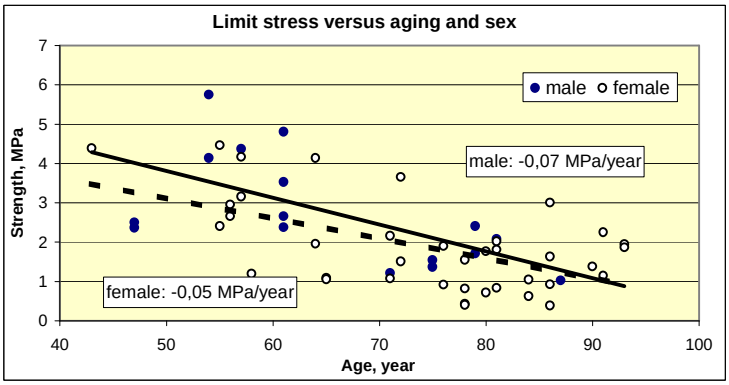

Figure 6. Linear approximation of age-related decline of limit stress of vertebrae L1-L2

Mosekilde [17] emphasized that a basic understanding of age-related changes in the quality and strength of vertebral bone is crucial. Based on his combinative study he demonstrated that age is the major determinant of vertebral bone strength, mass, and microarchitecture. There is, after the age of 50 years, a higher tendency for disconnection of the trabecular network in women than in men.

By applying linear approximation, the decrease trends of the strength characteristics can be calculated numerically. Table 4 contains the values of decrease trends for a year of aging, related to the total analyzed age span, for the main strength parameters, that is, break loads, limit stresses, Young's moduli and energy absorption capacity.

Table 4. Numerical decrease trends of compressive mechanical characteristics with aging

Lumbar vertebrae L1-L2		Males	Females	Total
Break load	N/year	-90	-56	-80
Limit stress	Mpa/year	-0.07	-0.05	-0.06
Young modulus	Mpa/year	-2.8	-1.7	-2.1
Energy absorption	Joule/year	-0.029	-0.022	-0.028

It can be observed in Table 4 that the decrease trends of women are smaller than those of men. The decrease trends of women are about 60% of those of men, equally for break load, limit stress Young's modulus and energy absorption capacity.

For sex-independent analysis, for the total group, by applying linear approximation for the total age interval 43-93 years, for break load, the approximate mean decrease trend can be considered to be -80 N for a year of aging. For limit stresses, the approximate mean decrease trend can be considered to be -0.06 MPa/year, for compressive Young's moduli -2.1 MPa/year, for energy absorption capacity -0.028 Joule/year.

As a conclusion of our experiments, during the age period between 40-90 years, the strength properties decrease by 60-70% for both sexes. According to the linear regression analysis of McCaldren et al [14] related to the age-dependent changes in the compressive strength of cancellous bone of 255 femoral cadaver specimens from donors in age of 20 to 102 years, the compressive strength decrease yields 8,5% in each decade of aging. This means that the 80 years long decrease period yields 68% of total strength decrease. Mosekilde [16] also mentioned that the decline in strength of the whole vertebral body during normal aging for both men and women is 70-80%. These results are in agreement with our results.

Table 5 contains the correlation coefficients of all compressive mechanical strength characteristics with aging for males and females, respectively.

Table 5. Correlation between strength characteristics and aging

Male / **Female**	Age	Break load	Limit stress	Limit strain	Young's mod.	Prop. stress	Energy absorb.
Age	**1.0**	-0.57	-0.62	-0.00	-0.55	-0.64	-0.37
Break load	-0.52	**1.0**	0.9	-0.05	0.95	0.95	0.80
Limit stress	-0.57	0.97	**1.0**	0.03	0.96	0.98	0.80
Limit strain	-0.12	0.11	0.13	**1.0**	-0.18	0.01	0.25
Young's modulus	-0.52	0.86	0.91	-0.17	**1.0**	0.93	0.72
Proportional stress	-0.55	0.93	0.97	0.13	0.86	**1.0**	0.68
Energy absorption	-0,51	0.78	0.76	0.35	0.62	0.64	**1.0**

Obviously, there is a negative correlation between the compressive strength parameters and aging for both sexes, since the load-bearing capacity decreases with aging. The age-dependence in the proportional and limit stresses and in the Young's moduli is slightly larger for men than for women. However, practically, there is no correlation with aging in strains for men, and only a small correlation is found for women. The age-dependence of energy absorption capacity seems to be larger for women than for men.

These results agree with the results of Mori [15] who found the correlation between aging and compressive Young's modulus of normal patients to be -0.527, based on compression tests of bone samples of vertebra L3. Similarly, based on compressive tests of lumbar vertebrae, Tanaka et al. [18] found the correlation significant, namely, -0.66 between limit stresses and aging.

3.2. **Trabecular bone architecture of lumbar vertebrae.** Bone architecture and bone mineral density are in close relation with each other. Figure 7 illustrates the age-related decrease of the areal bone mineral density (aBMD) of the measured vertebrae, by distinguishing between the sexes. It can be observed that in the age period of the experiment (43-93 years) the analyzed vertebrae belong to the strongly osteoporotic group, moreover, women are in an advanced osteoporotic state, having lower bone mineral density than men. It can be concluded that the areal bone mineral density decreases significantly with aging. The decrease trend can be numerically verified by applying linear approximation.

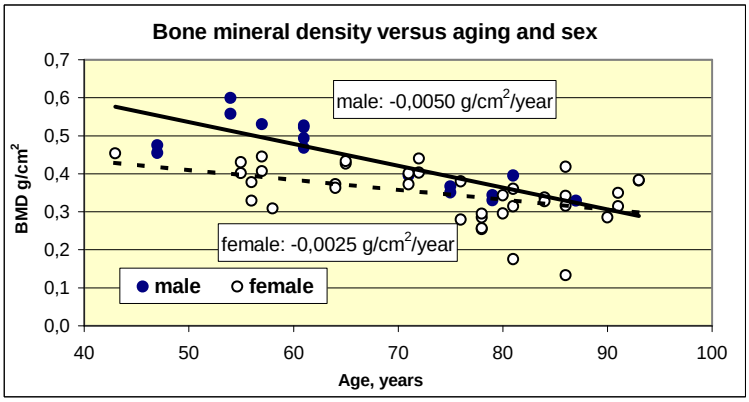

Figure 7. Age-related decline of areal bone mineral density of vertebrae L1-L2

Obviously, all compressive strength parameters increase significantly with bone mineral density, or, inversely, decrease significantly with the age-related decrease of aBMD.

Figure 8 illustrates the age-related weakening of trabecular architecture, namely, the loss of trabecular diameter and the parameters of several trabecular areal ratios.

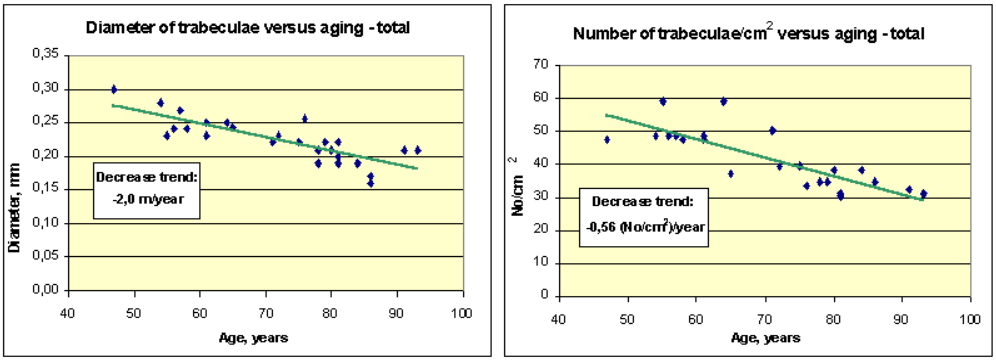

Figure 8. Age-related decrease of trabecular architecture of vertebrae L1-L2

Linear approximation of age-dependence of trabecular diameters, and areal ratio of trabecular bone are illustrated.

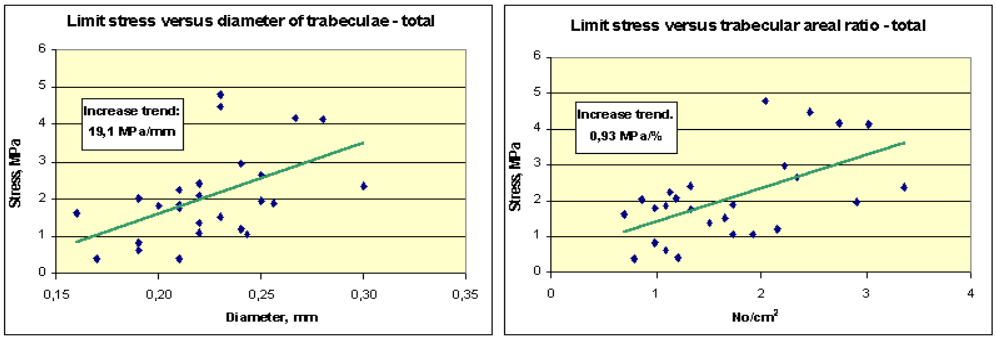

Figure 9. Increase of limit stress versus trabecular architecture of vertebrae L1-L2

In Figure 9 the linear approximation of the increase of limit stress in terms of the diamater and areal ratio of trabeculae is illustrated. It verifies numerically the effect of trabecular weakening on the compressive strength of vertebrae in osteoporosis.

4. **Summary**

Tension and compression analysis of the human lumbar spine was presented. Based on in vivo experiments, a parameter-dependent viscoelastic numerical tensile model of lumbar-lumbosacral functional spinal units was created for numerical simulations of traction therapies. At the sane time, in vitro compression tests and CT morphometry of lumbar vertebrae were compared to obtain the relation between the compressive load bearing capacity and bone architecture of osteoporotic segments.

For the numerical creep models of human lumbar-lumbosacral segments L3-S1, elastic and damping moduli have been calculated for tension. By means of the initial elastic moduli and the damping parameters, it has been numerically shown that the rigidity of segments increases significantly with aging. Moreover, the time related difference between the deformation propagation in male and female patients depends on the different damping properties of sexes. The values of elastic and creep parameters are approximate, since they are very sensitive to the measured deformations. However, their ratio and tendency provide very important information for the numerical simulation of traction therapies. The numerical simulation and parameter-identification of human lumbar spine segments were presented in centric tension. 2D and 3D FEM models were used, and the global elongations of FSUs were used for identification of the local material parameters of the component organs of lumbar spine segments.

Since there are no in vivo experimental results in the international literature for the human lumbar spine segments or discs in pure centric tension when the effect of muscles can be excluded, the results presented may attract the interests of the biomechanical analysts of the human lumbar spine.

The compressive strength of osteoporotic lumbar vertebrae has been measured in vitro, in terms of aging, sex and bone architecture. It has been concluded that the load-bearing capacity decreases with aging, thus, there is a significant negative correlation between compressive strength parameters and aging for both sexes. By applying linear approximation for age-dependence, the decrease trends of compressive strength characteristics were calculated numerically. Bone mineral density and the parameters of trabecular bone loss were compared with the measured compressive strength characteristics.

Acknowledgement. The present study has been supported by the projects OTKA T/022622, T033020, T046755, ETT- 257/2000.

REFERENCES

1. Kurutz, M., Bene, E., Lovas, A., Molnár, P. and Monori, E.: Extension of the lumbar spine, measured during weightbath therapy, (In Hung.), *Orvosi Hetilap*, **143**(13), (2002), 673-684.
2. Kurutz, M., Bene, E., Lovas, A., Monori, E. and Molnár, P.: In vivo deformability of human lumbar spine segments in pure centric tension, measured during traction bath therapy. *Acta of Bioengineering and Biomechanics*, **4**(Suppl.1), (2002), 219-220.
3. Bene, E. and Kurutz, M.: Application and biomechanics of traction bath, (in Hung.), Orvosi Hetilap, **134**, (1993), 1123-11293.
4. Moll, K.: Treatment of discus hernia with so-called "weightbath" therapy. (In Hung.), *Orvosi Hetilap*, **94**, (1953), 123-126.
5. Kurutz, M.: Die Behandlung der Discushernien mit den sogenannten "Gewichtsbadern". *Contempl. Rheum.*, **97**, (1956), 326-329.
6. Moll, K.: The role of traction therapy in the rehabilitation of discopathy. *Rheum. Balneol. Allerg.*, **3**, (1963), 174-177.
7. Bene, E.: Das Gewichtbad, *Z. Phys. Med. Baln. Klim.*, **17**, (1988), 67-71.

8. Kurutz, M., Bene, E. and Lovas, A.: In vivo deformability of human lumbar spine segments in pure centric tension, measured during traction bath therapy. *Acta of Bioengineering and Biomechanics*, **5**(1), (2003), 67-92.
9. Antosik, T. and Awrejcewicz, J.: Numerical and experimental analysis of biomechanics of three lumbar vertebrae. *Journal of Theoretical and Applied Mechanics*, **3**, (1999), 37.
10. Ciach, M. and Awrejcewicz, J.: Finite element analysis and experimental investigations of the intervertebral discs in the human and porcine lumbar spinal segment, Proc. Conf. Biomech. Modelling, Computational Meth., Experiments and Biomedical Applications, Lodz, Dec. 7-8. 1998.
11. Ciach, M., Maciejczak, A., Awrejcewicz, J. and Radek, A.: A comparison of two surgical techniques using finite element model of cervical spine before and after discectomy with interbody bone graft, Proc. Conf. Biomech. Modelling, Computational Meth., Experiments and Biomedical Applications, Lodz, Dec. 7-8. 1998.
12. Hansson, T.H., Keller, T.S. and Panjabi, M.M.: A study of the compressive properties of lumbar vertebral trabeculae: effects of tissue characteristics. *Spine*, **12**, (1987), 56.
13. Lindahl, O.: Mechanical properties of dried defatted spongy bone, *Acta Orthop. Scand.*, **47**, (1976), 11.
14. McCaldren, R.W., McGeough, J.A. and Court-Brown, C.M.: Age-related changes in the compressive strength of cancellous bone. The relative importance of changes in density and trabecular architecture. *Bone Joint Surg. Am.*, **79**(3), (1997), 421-427.
15. Mori, S.: Effect of aging on compressive strength of lumbar trabecular bone in hemodialyzed and non-hemodialyzed patients. *Nippon Jinzo Gakkai Shi.*, **36**(6), (1994), 752-761.
16. Mosekilde, L.: The effect of modelling and remodelling on human vertebral body architecture. *Technol. Health Care*, **6**(5-6), (1998), 287-297.
17. Mosekilde, L.: Age-related changes in bone mass, structure, and strength effects of loading. *Z. Rheumatol.*, **59**(Suppl.1), (2000), 1-9.
18. Tanaka, Y., Kokubun, S., Sato, T., Iwamoto, M. and Sato, I.: Trabecular domain factor and its influence on the strength of cancellous bone of the vertebral body. *Calcif. Tissue Int.*, **69**, (2001), 287-292